CARPATHIAN J. MATH.
Volume **41** (2025), No. 2,
Pages 329-349

Online version at https://www.carpathian.cunbm.utcluj.ro/
ISSN 1584-2851 (Print edition); ISSN 1843-4401 (Electronic)
DOI: https://doi.org/10.37193/CJM.2025.02.05

Stability and bifurcations in an epidemic model with nonlinear transmission and removal rates

RALUCA EFREM, MIHAELA STERPU, AND DANA CONSTANTINESCU

ABSTRACT. A generalized SEIR epidemiological model, incorporating general nonlinear transmission and removal rates, has been developed and investigated. Local and global stability theory and bifurcation theory are used to determine the dynamics of the model. The presence of unique or coexisting attractors is proved and different scenarios for the evolution of the model, towards a stable equilibrium point or a limit cycle are found. The theoretical results are supported by numerical simulations, obtained using Holling type II functions.

1. INTRODUCTION

In recent years, attempts have been made to develop realistic mathematical models for infectious disease transmission dynamics. The aims of developing such models are to understand the observed epidemiological patterns and predict the outcome of the introduction of public health interventions to control the spread of the disease. The model's capacity to predict disease control, on the other hand, is highly dependent on the assumptions made throughout the modeling process.

The SEIR (Susceptible Exposed Infectious Recovered) model is one of the most widely used mathematical models for describing epidemic dynamics and predicting potential transmission scenarios. In this paper we propose and analyze an updated version of the epidemic prediction model based on the SEIR approach, using generalized nonlinear and infection dependent functions for both the transmission and the removal rates.

The incidence rate (the rate of new infections) is regarded to be crucial in communicable disease modeling in order to guarantee that the model delivers an appropriate qualitative representation of the dynamics of the disease [1], [2], [3], [4], [5], [6]. In most conventional disease transmission models, the incidence rate is defined as mass action incidence with bilinear interactions, given by βIS, where β is the probability of infection per contact, while S and I represent the susceptible and infected populations, respectively.

The use of saturating and nearly bilinear incidence rates, among other nonlinear incidence rates, is justifiable practically. For instance, Yorke and London [7] showed that the incidence rate $\beta(1 - cI)IS$, with positive c and time dependent β, is consistent with the outcomes of measles epidemic simulations. Capasso and Serio [2] employed a saturated incidence rate $\beta(1 + \beta\delta I)IS$, $\delta > 0$, in order to avoid contact rate unboundedness. To account for behavioral changes, Liu and colleagues [8], [9] employed a nonlinear incidence rate given by $\frac{kI^lS}{1+\alpha I^h}$, where $k, l, \alpha, h > 0$. The literature is replete with models with nonlinear incidence rates (see [6] for a basic overview).

Recent theoretical and clinical research have also put forth several explanations for the nonlinearity of the incidence rates, including non-constant rates of contact between an infected person and another person in the population ([4], [5], [10], [11], [12], [13],

Received: 07.12.2013. In revised form: 15.10.2024. Accepted: 30.10.2024
2010 *Mathematics Subject Classification.* 37G35, 34C23, 37M05.
Key words and phrases. *SEIR model, stability, bifurcation, nonlinear transmission rate, nonlinear removal rate.*
Corresponding author: Raluca Efrem; raluca.efrem@edu.ucv.ro

[14]). These studies have demonstrated, with biological justifications, that the contact rate may change depending on factors such as behavioral changes, an increase in the risk of infection from multiple exposures, the severity of the infection, the recruitment of infected people, or the stage of the infection.

More recent studies on epidemiological models with incidence of mass action, have initially included a fixed rate of removal corresponding to a maximum capacity of resources for treatment in a community [15], [16], [17], [18], [19]. Although this method should be implemented as soon as an epidemic starts, given the public health resources at hand, it might not be immediately viable to operate at full capacity. Additionally, with such a strategy in place and the resources used, it is normal to anticipate that the removal rate of infected people will decline as the number of infected people rises. Considering an approach that allows for a varied elimination rate in line with various stages of an epidemic seems therefore more practical.

The model we propose and analyze generalizes a basic SEIR model, by means of using the transmission rate $\beta(1+f(I,\nu))I$ and the removal rate $\gamma+g(I,k)$, with f,g nonlinear functions, satisfying certain conditions. The dynamics of the model is analyzed using local and global stability theory of nonlinear systems of differential equations. The results of the study show the existence of several different scenarios for the evolution of the model, either to the disease free equilibrium point, or to an endemic equilibrium, or even to a periodic behavior.

The numerical simulations, performed using Matlab (R2014a) and Maple 18 (Waterloo Maple Maplesoft), support the theoretical results.

The paper is organized as follows. In section 2 the model analyzed in this paper is formulated and some qualitative properties are proved. In the subsequent sections we discuss several theoretical aspects of the model: we determine the basic reproduction number and the equilibrium points of the model, we investigate the local and global stability, and we analyze the codimension one local bifurcations of the model. Next, we illustrate the theoretical results using type II Holling response functions for the nonlinear infection dependent transmission and removal rates. Finally, we summarize our results and draw some conclusions.

2. The model

2.1. **The model formulation.** We propose a modified SEIR model, given by the following set of nonlinear differential equations:

$$\begin{aligned}
\frac{dS}{dt} &= A-\beta(1+f(I,\nu))IS-\mu S\\
\frac{dE}{dt} &= \beta(1+f(I,\nu))IS-\alpha E-\mu E\\
\frac{dI}{dt} &= \alpha E-(\gamma+g(I,k))I-\mu I\\
\frac{dR}{dt} &= (\gamma+g(I,k))I-\mu R
\end{aligned} \tag{2.1}$$

with the initial conditions $S(0)>0$, $E(0)\geq 0$, $I(0)\geq 0$, $R(0)\geq 0$. The significance of the state variables and parameters are given in Tables 1, 2 below. We assume that infectious disease causes permanent immunity.

TABLE 1. Variables of the model

Variable	Description
$N(t) = S(t) + E(t) + I(t) + R(t)$	total population
$S(t)$	susceptible population
$E(t)$	exposed population
$I(t)$	infected population
$R(t)$	removed population

TABLE 2. Parameters of the model

Parameter	Description
A	recruitment rate of the population
β	probability of infection per contact per unit time
μ	natural death rate
α	inverse of the average incubation period
γ	inverse of the average duration of infection

The incidence rate is $\beta(1 + f(I, \nu))IS$, where $f(I, \nu)$ is a positive, nonlinear, differentiable function for $I, \nu \geq 0$, satisfying the following assumptions:

$$\begin{aligned} &(H1) \quad f(0, \nu) = f(I, 0) = 0, \\ &(H2) \quad \frac{\partial f}{\partial I} > 0, \\ &(H3) \quad \frac{\partial^2 f}{\partial I^2} \leq 0, \end{aligned} \tag{2.2}$$

for $I > 0$.

The nonlinear factor f predominates when ν and I are large enough, as shown by (H1), whereas the bilinear term predominates when ν or I are small. As a result, since it reduces the infection rate to βIS when it became null, ν can be viewed as a metric that measures departure from mass action (see [20]).

The hypotheses (H1)-(H3) are satisfied by a large number of functions, such as (i) $f(I, \nu) = \nu I^q$, with $0 < q \leq 1$ and $\nu > 0$ (Example 4.1 in [20]); (ii) $f(I, \nu) = \frac{\nu I^q}{1+\nu I^q}$ or $f(I, \nu) = \frac{\nu I^q (1+kI)^p}{1+\nu I^q}, p + q = 1, p, q, k \geq 0$ (Example 4.2 in [20]); (iii) $f(I, \nu) = 1 - e^{-\nu I}, \nu > 0$.

The infection dependent removal rate $\gamma + g(I, k)$ is dependent on a nonlinear function g. The variable k, named elimination rate, depends on the number of infected people. Here k is defined as the maximum capacity for removing infected persons, the removal rate is anticipated to decrease as the number of illnesses grows. Therefore we consider a positive differentiable function $g(I, k)$, for $I, k \geq 0$, which satisfies the following general assumptions:

$$\begin{aligned} &(H4) \quad g(0, k) = k, g(I, 0) = 0, \\ &(H5) \quad \frac{\partial g}{\partial I} < 0, \\ &(H6) \quad \frac{\partial^2 g}{\partial I^2} \geq 0, \end{aligned} \tag{2.3}$$

for $I > 0$.

The function $g(I, k) = \frac{k}{1+cI^r}$ for $0 < r \leq 1$, $c > 0$, (as in the example in [21]) satisfies (H4)-(H6).

Since R does not appear in the first three equations of the system (2.1), it reduces to the

following three-dimensional system:

$$\begin{aligned}\frac{dS}{dt} =& A-\beta(1+f(I,\nu))IS-\mu S\\ \frac{dE}{dt} =& \beta(1+f(I,\nu))IS-\alpha E-\mu E\\ \frac{dI}{dt} =& \alpha E-(\gamma+g(I,k))I-\mu I.\end{aligned} \tag{2.4}$$

Denote by $x\left(t\right)=\left(S(t),E(t),I(t)\right)^{T}$ and by X the vector field associated with this system (2.4), $X\left(S,E,I\right)=\left(X_1,X_2,X_3\right)^{T}$, with $X_1=A-\beta(1+f(I,\nu))IS-\mu S$, $X_2=\beta(1+f(I,\nu))IS-\alpha E-\mu E$, $X_3=\alpha E-(\gamma+g(I,k))I-\mu I$. System (2.4) is as follows

$$\dot{x}\left(t\right)=X\left(x(t)\right).$$

Denoting by $y\left(t\right)=\left(S(t),E(t),I(t),R(t)\right)^{T}$ and by Y the vector field associated with this system (2.4), $Y\left(S,E,I,R\right)=\left(X_1,X_2,X_3,X_4\right)^{T}$, with $X_4=(\gamma+g(I,k))I-\mu R$, system (2.1) reads

$$\dot{y}\left(t\right)=Y\left(y(t)\right).$$

2.2. **Qualitative behavior of the model.**

2.2.1. *Positivity.* Denoting $e_1=\left(1,0,0\right)$, $e_2=\left(0,1,0\right)$, and $e_3=\left(0,0,1\right)$ the normal vectors of the planes $S=0$, $E=0$, and $I=0$, respectively, we obtain $\langle X,e_1\rangle_{|S=0}=A>0$, $\langle X,e_2\rangle_{|S\geq0,E=0,I\geq0}=\beta(1+f(I,\nu))IS\geq0$, $\langle X,e_3\rangle_{|S\geq0,E\geq0,I=0}=\alpha E\geq0$. Applying Nagumo's Theorem ([22], [23]), it follows that the region

$$\mathbb{R}^3_+=\{(S,E,I)|S\geq0,E\geq0,I\geq0\} \tag{2.5}$$

is a positively invariant set for the system (2.4).

In addition, as $X_4=(\gamma+g(I,k))I\geq0$ for $R=0$, $S\geq0,E\geq0,I\geq0$, the set

$$\mathbb{R}^4_+=\{(S,E,I,R)|S\geq0,E\geq0,I\geq0,R\geq0\} \tag{2.6}$$

is a positively invariant set for the system (2.1).

2.2.2. *Boundedness.* Summing the equations in (2.1) we obtain $\frac{dN}{dt}=A-\mu N$, thus $N\left(t\right)=\frac{A}{\mu}+\left(N\left(0\right)-\frac{A}{\mu}\right)e^{-\mu t}$. As $\lim\limits_{t\to\infty}N(t)=\frac{A}{\mu}$, it follows that

$$\lim_{t\to\infty}\sup(S(t)+E(t)+I(t)+R(t))\leq\frac{A}{\mu}.$$

It follows the attractors in $\mathbb{R}^3_+$ of the dynamical system associated with (2.4) are included in the region:

$$\Gamma=\{(S,E,I)|S>0,E\geq0,I\geq0,S+E+I\leq\frac{A}{\mu}\}. \tag{2.7}$$

3. Basic Reproduction Number and Equilibrium Points

3.1. **The basic reproduction number.** The predicted number of secondary cases that a typical infected individual will create in a population that is entirely susceptible is known as the basic reproduction number, or R_0. If $R_0<1$, then an infected person typically infects less than one additional person during the course of their infectious period, and the infection cannot spread. On the other hand, if $R_0>1$, each sick person creates, on average, more than one new infection, and the disease can spread across the community.

Thus, the conditions under which the disease spreads can be calculated by determining R_0 as a function of the model parameters. In the case of a single infected compartment, R_0

is just the product of the infection rate and its average duration. It is frequently possible to locate an exact formula for R_0 when the model is simple [24].

The next-generation matrix approach was created by Diekmann et al. [25] to determine the fundamental reproduction number R_0, then Van den Driessche and Watmough [24] modified it. This algorithm denotes the vector of states by x and the disease free equilibrium by x_0. For each infected compartment i, $F_i(x)$ is the rate of appearance of new infections in compartment i and $V_i(x)$ is obtained as the difference between the rate of transfer of individuals out of compartment i and the rate of transfer of individuals into compartment i by all other means. Then

$$\frac{dx_i}{dt} = F_i(x) - V_i(x)$$

Let **F** and **V** by the Jacobian matrix of F and V in x_0, i.e.

$$\mathbf{F}_{ij} = \frac{\partial F_i(x)}{\partial x_j} \mid x = x_0 \tag{3.1}$$

$$\mathbf{V}_{ij} = \frac{\partial V_i(x)}{\partial x_j} \mid x = x_0 \tag{3.2}$$

The matrix $\mathbf{FV}^{-1}$ is called the next generation matrix. Then, R_0 is defined to be the spectral radius of the matrix $\mathbf{FV}^{-1}$.
In the case of model (2.4) there are two infected compartments, I and E. Choosing

$$F = \begin{pmatrix} \beta(1+f(I,\nu))IS \\ \alpha E \end{pmatrix}, \quad V = \begin{pmatrix} (\alpha+\mu)E \\ (\mu+\gamma+g(I,k))I \end{pmatrix},$$

we have

$$\mathbf{F} = \begin{pmatrix} 0 & \frac{\beta A}{\mu} \\ \alpha & 0 \end{pmatrix}, \quad \mathbf{V} = \begin{pmatrix} \alpha+\mu & 0 \\ 0 & \mu+\gamma+k \end{pmatrix}.$$

So, the basic reproduction number R_0 for the model (2.4) is obtained as

$$R_0 = \sqrt{\frac{\alpha\beta A}{\mu(\alpha+\mu)(\gamma+\mu+k)}}$$

In the literature the square root is omitted as it gives the same threshold for stability at $R_0 = 1$. Thus we shall consider

$$R_0 = \frac{\alpha\beta A}{\mu(\alpha+\mu)(\gamma+\mu+k)}. \tag{3.3}$$

3.2. **Equilibrium points of the model.** The equilibria of system (2.4) satisfy

$$\begin{aligned} A - \beta(1+f(I,\nu))IS - \mu S &= 0 \\ \beta(1+f(I,\nu))IS - \alpha E - \mu E &= 0 \\ \alpha E - (\gamma + g(I,k))I - \mu I &= 0 \end{aligned} \tag{3.4}$$

which reduces to

$$\begin{aligned} S &= \frac{A}{\beta(1+f(I,\nu))I + \mu} \\ E &= \frac{(\gamma+\mu+g(I,k))I}{\alpha} \\ \frac{A\beta(1+f(I,\nu))I}{\beta(1+f(I,\nu))I+\mu} &= \frac{(\alpha+\mu)}{\alpha}(\gamma+\mu+g(I,k))I \end{aligned} \tag{3.5}$$

Notice that, in the absence of the disease ($I = 0$), the model (2.4) has an uninfected steady state $P_0 = (\frac{A}{\mu}, 0, 0)$, called the disease-free equilibrium point, which exists for all parameter values.

Performing a simple calculation, one can obtain the endemic equilibrium points $P = (S^*, E^*, I^*)$ of the model (2.4), with

$$\begin{aligned} S^* &= \frac{A}{\beta(1+f(I^*,\nu))I^* + \mu} \\ E^* &= \frac{(\gamma+\mu+g(I^*,k))I^*}{\alpha} \end{aligned} \tag{3.6}$$

and I^* is a positive fixed point of the function

$$\Phi(I) = \frac{\mu}{\beta}\left(R(I,k) - \frac{1}{1+f(I,\nu)}\right), \tag{3.7}$$

where

$$R(I,k) = \frac{\alpha\beta A}{\mu(\alpha+\mu)(\gamma+\mu+g(I,k))}. \tag{3.8}$$

So the number of the endemic equilibrium points corresponds to the number of the fixed points of the function (3.7). We are going to assume that:

$$(H7) \quad \frac{\partial^2 R}{\partial I^2} \leq 0 \tag{3.9}$$

which is a sufficient condition for Φ to be a concave function, with respect to the variable I.

Note that $R(0,k) = R_0$.

Lemma 3.1. *Assume that the hypotheses (H1)-(H7) are satisfied. Then the function Φ has the following properties:*
(i) $\Phi(0) = \frac{\mu}{\beta}(R_0 - 1) \overset{not.}{=} \Phi_0$;
(ii) $\frac{d\Phi}{dI} > 0$ *for* $I > 0$;
(iii) $\frac{d^2\Phi}{dI^2} \leq 0$ *for* $I > 0$;
(iv) $\lim_{I\to\infty} \Phi(I) \overset{not.}{=} \Phi_\infty < \infty$.

Proof. (i) We have $\Phi(0) = \frac{\mu}{\beta}(R(0,k) - \frac{1}{1+f(0,\nu)}) = \frac{\mu}{\beta}(R_0 - 1)$.
(ii) Differentiating (3.8) we obtain $\frac{\partial R}{\partial I} = -\frac{A\alpha\beta}{\mu(\mu+\alpha)(\mu+\gamma+g(I,k))^2}\frac{\partial g}{\partial I} > 0$, using (H5). This implies that $\frac{d\Phi}{dI} = \frac{\mu}{\beta}(\frac{\partial R}{\partial I} + \frac{1}{(1+f(I,\nu)^2}\frac{\partial f}{\partial I}) > 0$, taking into account the hypothesis (H2).
iii) For the second derivative of Φ we obtain

$$\frac{d^2\Phi}{dI^2} = \frac{\mu}{\beta}\left(\frac{\partial^2 R}{\partial I^2} - \frac{2}{(1+f(I,\nu))^3}\left(\frac{\partial f}{\partial I}\right)^2 + \frac{1}{(1+f(I,\nu))^2}\frac{\partial^2 f}{\partial I^2}\right) \leq 0$$

due to (H3) and (H7).
iv) Since f is a positive, increasing function, it follows that $\lim_{I\to\infty} f(I,\nu)$ can be either a finite number $f_\infty(\nu)$ or $+\infty$. Thus

$$\Phi_\infty = \begin{cases} \frac{A\alpha}{(\mu+\alpha)(\mu+\gamma+g_\infty(k))}, & \text{if} \quad \lim_{I\to\infty} f(I,\nu) = +\infty \\ \frac{\mu}{\beta}\left(\frac{A\alpha\beta}{\mu(\mu+\alpha)(\mu+\gamma+g_\infty(k))} - \frac{1}{1+f_\infty(\nu)}\right), & \text{if} \quad \lim_{I\to\infty} f(I,\nu) = f_\infty(\nu) \end{cases}$$

where $g_\infty(k) = \lim_{I\to\infty} g(I,k)$. We conclude that $\Phi_\infty < +\infty$. □

Remark that if $R_0 = 1$, then $\Phi_0 = 0$, thus $I = 0$ is also a fixed point of Φ.

Lemma 3.2. *Assume that the hypotheses (H1)-(H7) are satisfied. Then:*
(i) if $\Phi_0 > 0$ then the function Φ has a unique positive fixed point;
(ii) if $\Phi_0 = 0$ then the function Φ has a unique positive fixed point if $\frac{d\Phi}{dI}(0) > 1$ and no positive fixed points, otherwise;
(iii) if $\Phi_0 < 0$ and $\Phi_\infty > 0$ then as $\frac{d\Phi}{dI}(0) > 1$, there exists a unique $\tilde{R}$ such that the function Φ may have no fixed point if $R_0 < \tilde{R}$, a unique fixed point if $R_0 = \tilde{R}$ and two fixed points if $\tilde{R} < R_0 < 1$, while as $\frac{d\Phi}{dI}(0) \leq 1$, there are no positive fixed points;
(iv) If $\Phi_0 < 0$ and $\Phi_\infty < 0$ then the function Φ has no fixed point.

Proof. From Lemma 3.1 we have $\frac{d\Phi}{dI} > 0, \frac{d^2\Phi}{dI^2} \leq 0, \lim_{I\to\infty} \Phi(I) = \Phi_\infty < \infty$ and $\Phi(0) = \frac{\mu}{\beta}(R_0 - 1)$. It follows that if $R_0 > 1$, then $\Phi(I)$ has a unique fixed point for $I > 0$ (see Fig. 1(iii), Fig. 2(v)).
Suppose $R_0 = 1$. Then, since $\Phi(0) = 0$, it follows that $\Phi(I)$ has a unique non-zero fixed point if $\frac{d\Phi}{dI}(0) > 1$ and no positive fixed points, otherwise (see Fig. 1(ii), Fig. 2(iv)).
If $\Phi_0 < 0$, then $R_0 < 1$. From the properties of Φ it follows that, for $I > 0$, $\frac{d\Phi}{dI}$ is a decreasing function, tending to 0 as $I \to \infty$. Since $\frac{d\Phi}{dI}(0) > 1$, there exists a unique value $\bar{I}$ such that $\frac{d\Phi}{dI}(\bar{I}) = 1$. If $\Phi(\bar{I}) > \bar{I}$, then Φ has two positive fixed points, if $\Phi(\bar{I}) = \bar{I}$, then Φ has one positive fixed point, while if $\Phi(\bar{I}) < \bar{I}$, then Φ has no positive fixed points. Denote

$$\bar{R} = \left(\frac{\beta}{\mu}\bar{I} + \frac{1}{1 + f\left(\bar{I}, \nu\right)}\right) \frac{\mu + \gamma + g\left(\bar{I}, k\right)}{\mu + \gamma + k}. \tag{3.10}$$

As $\Phi(I) = \frac{\mu}{\beta}\left(\frac{R_0(\mu+\gamma+k)}{\mu+\gamma+g(I,k)} - \frac{1}{1+f(I,\nu)}\right)$, it follows that if $R_0 < \bar{R}$, then $\Phi(\bar{I}) < \bar{I}$, if $R_0 = \bar{R}$, then $\Phi(\bar{I}) = \bar{I}$, while if $R_0 > \bar{R}$, then $\Phi(\bar{I}) > \bar{I}$. Hence the conclusion. As shown in Fig. 1(i), Fig. 2(i-iii), Fig. 3, $\Phi(I)$ may have at most two fixed points in this situation, corresponding to the points where the graph of function Φ intersects the first bisector. □

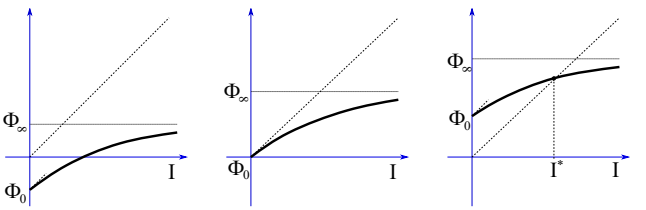

FIGURE 1. Graphics of Φ as a function of I, when $\frac{d\Phi}{dI}(0) \leq 1$.

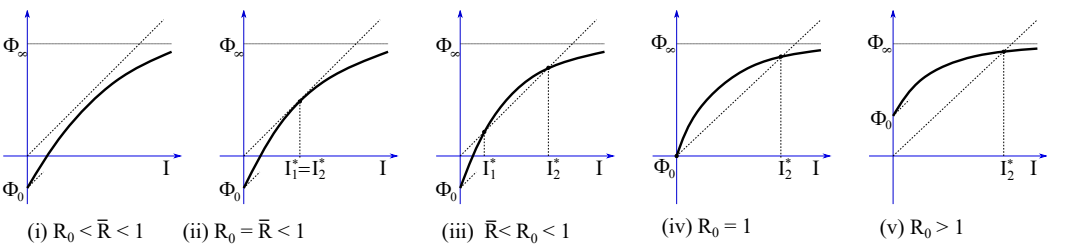

FIGURE 2. Graphics of Φ as a function of I, when $\frac{d\Phi}{dI}(0) > 1$.

The following theorems provide a summary of the results of this section.

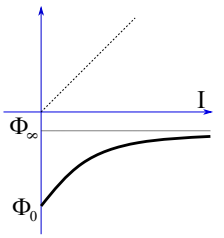

FIGURE 3. Graphics of Φ as a function of I, when $\Phi_\infty \leq 0$.

Theorem 3.1. *Assume* $\frac{d\Phi}{dI}(0) > 1$. *The following statements hold.*
(i) If $R_0 \geq 1$ *then the model (2.4) has a unique endemic equilibrium.*
(ii) If $R_0 < 1$ *and* $\Phi_\infty > 0$ *then there exists a unique* $\tilde{R}$ *such that the model (2.4) has no endemic equilibria if* $R_0 < \tilde{R}$, *a unique endemic equilibrium if* $R_0 = \tilde{R}$ *and two endemic equilibria if* $\tilde{R} < R_0 < 1$.
(iii) If $R_0 < 1$ *and* $\Phi_\infty < 0$ *then the model (2.4) has no endemic.*

Theorem 3.2. *Assume* $\frac{d\Phi}{dI}(0) \leq 1$. *The following statements hold.*
(i) If $R_0 > 1$ *then the model (2.4) has a unique endemic equilibrium.*
(ii) if $R_0 \leq 1$ *then the model (2.4) has no endemic equilibria.*

Proof. (i) If $R_0 > 1$ then $\Phi_0 > 0$ and using Lemma 3.2 (i) we conclude that there exists a unique equilibrium point.
(ii) If $R_0 = 1$ then $\Phi_0 = 0$ and the result follows from Lemma 3.2 (ii), as $\frac{d\Phi}{dI}(0) < 1$. Finally, if $R_0 < 1$ then $\Phi_0 < 0$ and the result follows from Lemma 3.2 (iii), as $\frac{d\Phi}{dI}(0) < 1$. □

Note that in the hypotheses $\tilde{R} < R_0 < 1$ and $\frac{d\Phi}{dI}(0) \geq 1$, two endemic equilibrium points coexist. Denote by I_1^*, I_2^* the positive fixed points of Φ in the case $\tilde{R} < R_0 < 1$, with $I_1^* < I_2^*$, and by I_2^* the unique positive fixed point of Φ in the case $R_0 > 1$. Also, denote by P_1 and P_2 the corresponding equilibria of system (2.4).

Remark 3.1. *As* $\frac{d\Phi}{dI}$ *is decreasing, in the case when there exists a unique endemic equilibrium, we have* $\frac{d\Phi}{dI}(I^*) < 1$. *In the case when there exist two endemic equilibria corresponding to* $I_1^* < I_2^*$, *we have* $\frac{d\Phi}{dI}(I_1^*) > 1$ *and* $\frac{d\Phi}{dI}(I_2^*) < 1$.

Remark 3.2. *As* $\tilde{R} = R_0 < 1$, *we have* $I_1^* = I_2^*$ *and* $\frac{d\Phi}{dI}(I_1^*) = 1$.

4. LOCAL AND GLOBAL STABILITY OF EQUILIBRIA

For an equilibrium point $P = (S^*, E^*, I^*)$, the Jacobian matrix is given by

$$J = \begin{pmatrix} -\beta(1+f(I^*,\nu))I^* - \mu & 0 & -\beta\left(\frac{\partial f}{\partial I}I^* + f(I^*,\nu) + 1\right)S^* \\ \beta(1+f(I^*,\nu))I^* & -\alpha-\mu & \beta\left(\frac{\partial f}{\partial I}I^* + f(I^*,\nu) + 1\right)S^* \\ 0 & \alpha & -\mu-\gamma-g(I^*,k) - \frac{\partial g}{\partial I}I^* \end{pmatrix} \tag{4.1}$$

and the corresponding characteristic polynomial reads

$$P(\lambda) = \lambda^3 + a_1(I^*)\lambda^2 + a_2(I^*)\lambda + a_3(I^*), \tag{4.2}$$

where

$$\begin{aligned} a_1(I^*) =& \beta I^* f(I^*,\nu) + \frac{\partial g}{\partial I}(I^*,k) I^* + \beta I^* + \gamma + g(I^*,k) + \alpha + 3\mu \\ a_2(I^*) =& -\frac{I^*(\alpha+\mu)(\gamma+g(I^*,k)+\mu)}{1+f(I^*,\nu)} \frac{\partial f}{\partial I}(I^*,\nu) + \\ &+ I^* \left[\beta I^*(1+f(I^*,\nu)) + \alpha + 2\mu\right] \frac{\partial g}{\partial I}(I^*,k) + \\ &+ (\gamma + g(I^*,k) + \alpha + 2\mu)\left[\beta I^*(1+f(I^*,\nu)) + \mu\right] \end{aligned} \tag{4.3}$$

and

$$\begin{aligned} a_3(I^*) =& -\frac{I^*\mu(\alpha+\mu)(\gamma+g(I^*,k)+\mu)}{1+f(I^*,\nu)} \frac{\partial f}{\partial I}(I^*,\nu) + \\ &+ I^*(\alpha+\mu)\left[\beta I^*(1+f(I^*,\nu)) + \mu\right] \frac{\partial g}{\partial I}(I^*,k) + \\ &+ I^*\beta(\alpha+\mu)(\gamma+g(I^*,k)+\mu)(1+f(I^*,\nu)) \\ =& -I^*\beta(\alpha+\mu)(\gamma+g(I^*,k)+\mu)(1+f(I^*,\nu)) \left[\frac{\mu}{\beta(1+f(I^*,\nu))^2} \frac{\partial f}{\partial I}(I^*,\nu) - \right. \\ &\left. - \frac{\beta I^*(1+f(I^*,\nu)) + \mu}{\beta(\gamma+g(I^*,k)+\mu)(1+f(I^*,\nu))} \frac{\partial g}{\partial I}(I^*,k) - 1\right]. \end{aligned} \tag{4.4}$$

4.1. **Stability of the disease-free equilibrium point.**

Theorem 4.3. *(i) If $R_0 < 1$ then the disease-free equilibrium point $P_0 = (\frac{A}{\mu}, 0, 0)$ is locally asymptotically stable.*
(ii) If $R_0 > 1$ then the disease-free equilibrium point P_0 is unstable, namely a saddle with a 2-dimensional locally stable manifold.
(iii) If $R_0 = 1$ then P_0 is a fold nonhyperbolic equilibrium point.

Proof. The Jacobian matrix at the disease-free equilibrium point $P_0 = (\frac{A}{\mu}, 0, 0)$ is

$$J_0 = \begin{pmatrix} -\mu & 0 & -\frac{A\beta}{\mu} \\ 0 & -\alpha-\mu & \frac{A\beta}{\mu} \\ 0 & \alpha & -\mu-\gamma-k \end{pmatrix}. \tag{4.5}$$

The characteristic polynomial associated with J_0 has one negative eigenvalue $\lambda_1 = -\mu < 0$ and the other two eigenvalues λ_2, λ_3 are the solutions of the equation: $\lambda^2 + b_1\lambda + b_2 = 0$, with

$$\begin{aligned} b_1 &= \gamma + \alpha + k + 2\mu > 0, \\ b_2 &= -(\alpha+\mu)(\gamma+\mu+k)(R_0-1). \end{aligned} \tag{4.6}$$

Using the sum and the product of the eigenvalues λ_2, λ_3 it is easy to determine their sign. Thus, as $R_0 < 1$, the equilibrium point is an attractor, while if $R_0 > 1$, P_0 is a saddle point of type $(n_s, n_u) = (2, 1)$.

Note that, as $R_0 = 1$, we have $\lambda_1 = -\mu, \lambda_2 = -(\gamma+\alpha+k+2\mu) < 0$, $\lambda_3 = 0$, thus P_0 is a nonhyperbolic equilibrium. □

Theorem 4.4. *The disease-free equilibrium point $P_0 = (\frac{A}{\mu}, 0, 0)$ is globally asymptotically stable on the region*

$$\Sigma = \{(S, E, I) \in \Gamma | \Phi(I) < 0\} \tag{4.7}$$

if (i) $\frac{d\Phi}{dI}(0) \leq 1$ and $R_0 < 1$ or (ii) $\frac{d\Phi}{dI}(0) > 1$ and $R_0 < \tilde{R}$.

Proof. Consider the Lyapunov function:

$$F = \alpha E + (\alpha + \mu) I. \tag{4.8}$$

The expression for the time-derivative of F is

$$\begin{aligned}\dot{F} &= \alpha \dot{E} + (\alpha + \mu)\dot{I} \\ &= \alpha \left[\beta(1 + f(I,\nu))IS - (\alpha + \mu)E\right] + (\alpha + \mu)\left[\alpha E - (\mu + \gamma + g(I,k))I\right] \\ &= \left[\alpha\beta(1 + f(I,\nu))S - (\alpha + \mu)(\gamma + g(I,k) + \mu)\right] I.\end{aligned}$$

Since $S \leq \frac{A}{\mu}$, it follows

$$\begin{aligned}\dot{F} \leq& \left[\alpha\beta(1 + f(I,\nu))\frac{A}{\mu} - (\alpha + \mu)(\gamma + g(I,k) + \mu)\right] I \\ =&(\alpha + \mu)(1 + f(I,\nu))(\gamma + \mu + g(I,k)) \\ &\times \left[\frac{A\alpha\beta}{\mu(\alpha + \mu)(\gamma + g(I,k) + \mu)} - \frac{1}{(1 + f(I,\nu))}\right] I \\ =&\frac{\beta}{\mu}(\alpha + \mu)(1 + f(I,\nu))(\gamma + \mu + g(I,k))\Phi(I)I.\end{aligned}$$

If $\Phi(I) < 0$ we have $\dot{F} < 0, \forall S, E, I > 0$. Let $W = \{(S, E, I) : \dot{F} = 0\}$. In the hypotheses (i) or (ii), there are no endemic equilibria it follows that $W = \{P_0\}$. Using LaSalle's invariance principle (see [26]), one can easily deduce that P_0 is globally asymptotic stable on Σ. □

As a consequence, when $\Phi_\infty < 0$, the disease free equilibrium P_0 is globally asymptotically stable if $R_0 < 1$.

4.2. **Stability of the endemic equilibria.**

Theorem 4.5. *(i) The endemic equilibrium point P_1 is unstable.*

(ii) The endemic equilibrium point P_2 is locally asymptotically stable if and only if

$$a_1(I_2^*) > 0 \text{ and } a_1(I_2^*)a_2(I_2^*) > a_3(I_2^*). \tag{4.9}$$

Proof. For an endemic equilibrium $P = (S^*, E^*, I^*)$, we have

$$\frac{A}{\beta(1 + f(I^*,\nu))I^* + \mu} = \frac{(\alpha + \mu)(\gamma + \mu + g(I^*,k))}{\alpha\beta(1 + f(I^*,\nu))}.$$

So, the coefficient a_3 of the characteristic polynomial (4.2) associated to the Jacobian matrix reads

$$a_3(I^*) = -I^*\beta(\alpha + \mu)(\gamma + g(I^*,k) + \mu)(1 + f(I^*,\nu))\left(\frac{d\Phi}{dI}(I^*) - 1\right). \tag{4.10}$$

According to the Hurwitz criterion [27], the characteristic equation has all solutions with negative real pars if and only if

$$a_1 > 0, a_3 > 0, a_1a_2 > a_3. \tag{4.11}$$

If $\frac{d\Phi}{dI}(I^*) > 1$, then $a_3 < 0$. Thus, it is not possible to have all three eigenvalues with negative real parts. Consequently, the endemic equilibrium P_1 is unstable. For the equilibrium P_2, we have $\frac{d\Phi}{dI}(I_2^*) \leq 1$, and the condition $a_3 > 0$ is satisfied, when $\frac{d\Phi}{dI}(I_2^*) \neq 1$ and $I_2^* \neq 0$. Thus, the equilibrium point P_2 is an asymptotically stable if conditions (4.9) are satisfied. □

5. Local bifurcations

For the general model (2.4), we prove that a transcritical bifurcation takes place as $R_0 = 1$, namely a backward bifurcation if $\frac{d\Phi}{dI}(0) > 1$ and a forward bifurcation if $\frac{d\Phi}{dI}(0) < 1$. Also, a fold bifurcation and a Hopf bifurcation at the endemic equilibrium points may occur.

5.1. **Transcritical bifurcation.** According to Theorem 4.3, as $R_0 = 1$, the disease-free equilibrium P_0 is non-hyperbolic. As $R_0 = 1$, the function Φ has a fixed point $I^* = 0$, namely I_1^* if $\frac{d\Phi}{dI}(0) > 1$ or I_2^* if $\frac{d\Phi}{dI}(0) \leq 1$. We prove the existence of a transcritical bifurcation by applying the Sotomayor Theorem [28], as mentioned in [29].

First, we have to choose a bifurcation parameter. Denote $\varepsilon = R_0 - 1$, thus $\varepsilon = 0$ is the bifurcation value.

As all the parameters are positive, we may express ε as a function of any of the parameters α, β, μ. As $\frac{\partial \varepsilon}{\partial \beta} = \frac{A\alpha}{\mu(\mu+\alpha)(\mu+\gamma+k)} > 0$, we can choose β variable and fix the other parameters, thus at $\varepsilon = 0$ we get that $\beta_0 = \frac{\mu(\alpha+\mu)(\gamma+k+\mu)}{A\alpha}$ is the corresponding threshold value. The Jacobian matrix at (P_0, β_0) has a simple zero eigenvalue and two negative eigenvalues $-\mu, -(\gamma + \alpha + k + 2\mu)$. The right and left eigenvectors corresponding to zero eigenvalue are

$$v = \begin{pmatrix} -\frac{(\alpha+\mu)(\gamma+k+\mu)}{\alpha\mu} \\ \frac{\gamma+k+\mu}{\alpha} \\ 1 \end{pmatrix}, \qquad w = \begin{pmatrix} 0 \\ \frac{\alpha}{\alpha+\mu} \\ 1 \end{pmatrix}. \tag{5.1}$$

It follows that

$$C_1 = \frac{1}{\langle v, w\rangle} w^T X_\beta(P_0, \beta_0) = 0, \tag{5.2}$$

$$C_2 = \frac{1}{\langle v, w\rangle} w^T \left[D^2 X(P_0, \beta_0)(v, v)\right] = \frac{2\beta(\gamma + k + \mu)}{\mu \langle v, w\rangle} \left(\frac{d\Phi}{dI}(0) - 1\right), \tag{5.3}$$

$$C_3 = \frac{2}{\langle v, w\rangle} w^T DX_\beta(P_0, \beta_0) v = \frac{2\alpha A}{\langle v, w\rangle (\alpha + \mu)\mu} \neq 0, \tag{5.4}$$

So, we have $C_2 > 0$ and $C_3 > 0$ if $\frac{d\Phi}{dI}(0) > 1$, while $C_2 < 0$ if $\frac{d\Phi}{dI}(0) < 1$. Defining the centre manifold variable y as the dynamics along v,

$$x(t) = P_0 + y(t)v,$$

the dynamics on the extended centre manifold is given by

$$\dot{y} = \varepsilon C_3 y + C_2 y^2. \tag{5.5}$$

Consequently, a transcritical bifurcation takes place on the centre manifold at $\varepsilon = 0$. The equilibria $y_1 = 0$, $y_2 = -\frac{C_3}{C_2}\varepsilon$ of equation (5.5) correspond to the equilibrium points P_0 and $P = (S^*, E^*, I^*)$, given, for small ε close 0, by

$$S^* = \frac{A}{\mu} + \frac{(\alpha+\mu)(\gamma+k+\mu)}{\alpha\mu}\frac{C_3}{C_2}\varepsilon, \qquad E^* = -\frac{\gamma+k+\mu}{\alpha}\frac{C_3}{C_2}\varepsilon, \qquad I^* = -\frac{C_3}{C_2}\varepsilon. \tag{5.6}$$

Note that condition $\varepsilon C_2 = C_2(R_0 - 1) < 0$ is necessary to ensure that the equilibrium P is located in Γ. We distinguish the following cases.

Case (i) If $C_2 > 0$, i.e. $\frac{d\Phi}{dI}(0) > 1$, the equilibrium $P \in \Gamma$ iff $R_0 < 1$; it follows that P coincides with P_1. Since y_2 is a repeller and y_1 is an attractor, we deduce that, close to $R_0 = 1$, the equilibrium P_1 is a saddle with a 2-dimensional stable manifold. Thus a backward bifurcation takes place.

Case (ii) If $C_2 < 0$, i.e. $\frac{d\Phi}{dI}(0) < 1$, the equilibrium $P \in \Gamma$ iff $R_0 > 1$; it follows that P coincides with P_2. Through the transcritical bifurcation, the equilibrium P_2 changes stability with P_0, thus, close to $R_0 = 1$, the equilibrium P_2 is an attractor. This is a forward bifurcation.

This discussion leads to the following result concerning the transcritical bifurcation.

Theorem 5.6. *The model (2.4) undergoes at $R_0 = 1$ a backward bifurcation if $\frac{d\Phi}{dI}(0) > 1$ and a forward bifurcation if $\frac{d\Phi}{dI}(0) < 1$.*

5.2. **Tangent bifurcation.** As Figure 2 suggests, a tangent bifurcation may take place as $R_0 = \bar{R}$. The characteristic polynomial (4.2) at the double endemic equilibrium $\bar{P} = (\bar{S}, \bar{E}, \bar{I})$ has at $R_0 = \bar{R}$ one of the eigenvalues equal to zero, as $a_3(\bar{I}) = 0$. The fold bifurcation is generic if the other two eigenvalues have non-zero real part, so if (i) $a_2\left(\bar{I}\right) \neq 0$ or (ii) $a_1(\bar{I}) \neq 0$ or (iii) $a_1(\bar{I}) = 0$ and $a_2(\bar{I}) < 0$. The conditions $C_1 \neq 0$, $C_2 \neq 0$ from the Sotomayor Theorem, computed as above, are difficult to prove analytically in this general setting.

5.3. **Hopf bifurcation.** The system (2.4) may undergo a Hopf bifurcation only at one of the endemic equilibrium points $P = (S^*, E^*, I^*)$ if the conditions

$$a_1(I^*) \neq 0, a_2(I^*) > 0, a_1(I^*)a_2(I^*) = a_3(I^*) \tag{5.7}$$

for the coefficients of the characteristic (4.2) are satisfied. These conditions ensure that the equilibrium point P is a Hopf singularity. Remark that for the endemic equilibrium P_2 we have, according to Theorem 4.5, $a_3\left(I_2^\star\right) > 0$. If conditions (5.7) are satisfied, then $a_1\left(I_2\right) > 0$, thus the centre manifold is attractive. As a consequence, if the conditions of the Andronov-Hopf bifurcation Theorem [30] are satisfied and a supercritical Hopf bifurcation takes place (i.e. the first Lyapunov coefficient is negative), then the stable limit cycle born through this bifurcation on the extended centre manifold is locally asymptotically stable. If such a situation occurs, the system dynamics would pass from the locally stable equilibrium P_2 to an attractive limit cycle, that is from a stable stationary state to a stable periodic behavior.

6. Case study

We illustrate in this section the theoretical results in the particular case when

$$f\left(I, \nu\right) = \frac{\nu I}{1 + \nu I}, \qquad g\left(I, k\right) = \frac{k}{1 + I},$$

with $\nu > 0$, and $k > 0$, as in [21]. Some simple computations show the assumptions (H1)-(H7) are true for this choice of functions. The stability and bifurcation results obtained theoretically in the previous sections were verified with a number of numerical simulations. We used the parameter values in Table 3, as in [21], [20], [31], [32], [33], and considered the parameters β and k variable for the bifurcation diagrams. The parameter strata of the static bifurcation diagram in the (β, κ)-plane, in Figure 4, are determined by the curves

$$\begin{aligned} T &= \left\{(\beta, k), \Phi\left(0\right) = 0\right\} = \left\{(\beta, k), \frac{\alpha A}{(\alpha + \mu)(\gamma + \mu + k)} - \frac{\mu}{\beta} = 0\right\}, \\ SN &= \left\{(\beta, k), \Phi(I^*) = I^*, \frac{d\Phi}{dI}(I^*) = 1\right\}. \end{aligned}$$

These curves determine three regions in the bifurcation diagram, with different number of equilibrium points:

TABLE 3. Parameter values used for computations.

Parameter	Value
A	0.5
β	in (0,0.05)
μ	0.02
α	0.456
γ	0.073
ν	0.01
κ	in (0,0.5)

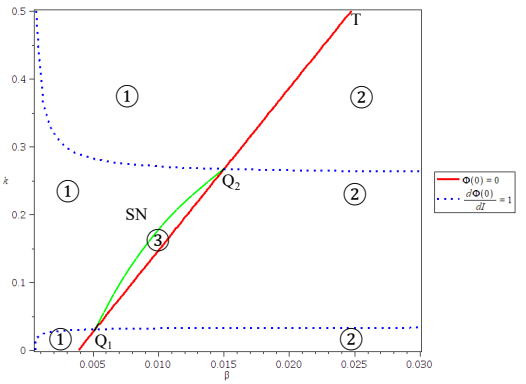

FIGURE 4. Static bifurcation diagram in the (β, k)-plane.

- in region 1 there exists only the disease free equilibrium P_0;

- in region 2 there exist two equilibria, the disease free equilibrium P_0, and the endemic equilibrium P_2;

- in region 3 there exist three equilibria, the disease free equilibrium P_0, and the endemic equilibria P_1, P_2;

- on SN there are 2 equilibria, P_0 and $P_1 = P_2$;

- on T, between the points Q_1 and Q_2 we have 2 equilibria, $P_0(= P_1)$ and P_2, while for the other parameter on T there exist only the disease free equilibrium $P_0(= P_2)$.

The characteristic polynomial

$$P(\lambda) = \lambda^3 + a_1(I^*)\lambda^2 + a_2(I^*)\lambda + a_3(I^*)$$

of Jacobi matrix for an endemic equilibrium point $P = (S^*, E^*, I^*)$ has the coefficients

$$\begin{aligned}
a_1(I^*) =& \frac{\beta\,(2\,\nu\,I^*+1)\,I^*}{\nu\,I^*+1} + \frac{k}{(1+I^*)^2} + \gamma + \alpha + 3\,\mu \\
a_2(I^*) =& \frac{-\beta A(2I^{*2}\nu^2 + 4I^*\nu + 1)\alpha}{(I^*\nu+1)(2I^{*2}\beta\nu + I^*\mu\nu + I^*\beta + \mu)} \\
&+ \frac{(2I^*\nu+1)I^*\left[(1+I^*)^2(\gamma+\alpha+2\mu)+k\right]\beta}{(I^*\nu+1)(1+I^*)^2} \\
&+ \frac{(\alpha+2\mu)k}{(1+I^*)^2} + (\alpha+2\mu)\gamma + \mu(2\alpha+3\mu) \\
a_3(I^*) =& \frac{-(2I^{*2}\nu^2 + 4I^*\nu + 1)\alpha\mu\beta A}{(I^*\nu+1)(2I^{*2}\beta\nu + I^*\mu\nu + I^*\beta + \mu)} \\
&+ \frac{(\alpha+\mu)(2I^*\nu+1)I^*\left[k+(\mu+\gamma)(1+I^*)^2\right])\beta}{(I^*\nu+1)(1+I^*)^2} \\
&+ \frac{(\alpha+\mu)\mu k}{(1+I^*)^2} + \mu(\alpha+\mu)(\mu+\gamma)
\end{aligned}$$

Taking into account the results in Section 5.3, for this choice of the functions f and g, system (2.4) may undergo a Hopf bifurcation at the endemic equilibrium P_2 provided the condition

$$a_1(I_2^*)a_2(I_2^*) = a_3(I_2^*)$$

is satisfied. Numerically we have determined two branches H_1, H_2 of parameters in the (β, k)-plane, analytically defined as

$$H_1 \cup H_2 = \left\{ (\beta, k)\,, \Phi(I_2^*) = I_2^*, \frac{d\Phi}{dI}(I_2^*) < 1, a_1(I_2^*)a_2(I_2^*) = a_3(I_3^*) \right\},$$

where Hopf bifurcation may occur. The static bifurcation diagram in Figure 4 is completed with the curves H_1 and H_2, containing parameter values where the endemic equilibrium point P_2 is a Hopf singularity, as illustrated in Figure 5. For parameter values inside the stratum between H_1 and H_2 (denoted as region 4 in Figure 5) the endemic equilibrium P_2 is unstable. Outside region 4, the equilibrium point P_2 as an attractor, where it exists. Note that region 4 intersects both regions 2 and 3. This means that a Hopf bifurcation may also take place for parameter values in region 3. Thus, for parameter values in region 3 there may coexist the locally attractive disease free equilibrium P_0 with either the attractive endemic equilibrium point P_2 or an attractive limit cycle.

We illustrate the dynamic behavior for two fixed values for the parameter k, namely $k = 0.2$ and $k = 0.4$. The values of β on the parameter strata SN, T, H_1, H_2 are given in Table 4. In order to establish the topological type of the equilibria P_1 and P_2, in Figure 6 we have represented the set $\mathcal{C} = \{(\beta, I)\,, \Phi\,(I) = I\}$ and its intersection with the bifurcation strata T, SN, $H_1 \cup H_2$ (denoted $T_{1,2}$, S, $H_{1,2}$, respectively), for two fixed values of the parameter k. Remark that the arc of $\mathcal{C}$ between points S and T_1 corresponds to I_1^*, while the arc starting from S and containing T_2 corresponds to I_2^*. For $k = 0.2$, the endemic equilibrium P_2 is an attractor when (I_2^*, β) is between S and H_1, it is unstable between H_1 and H_2, then it becomes an attractor after passing through H_2. For $k = 0.4$, the endemic equilibrium P_2 is an attractor when (I_2^*, β) is between T_2 and H_1, it is unstable between H_1 and H_2, then it becomes an attractor after passing through H_2.

We may summarize the information about the topological type of the equilibria for parameters (β, k) in the parameter portraits in Figures 4, 5 as follows:

- in region 1 the disease free equilibrium P_0 is an attractor;

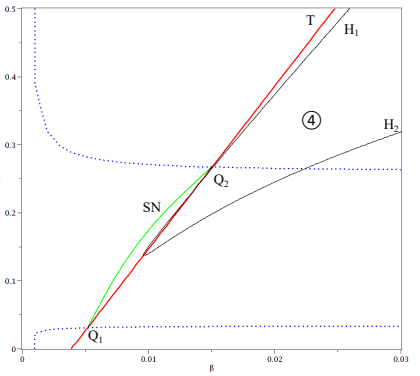

FIGURE 5. Dynamic bifurcation diagram in the (β, k)-plane.

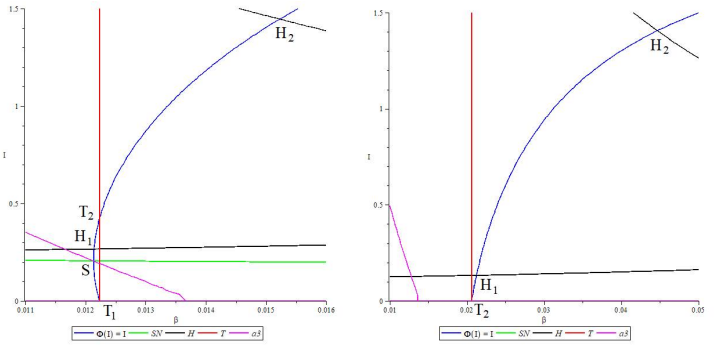

FIGURE 6. The curve $\Phi(I) = I$ in the (β, I)-plane and its intersection with the bifurcation strata, for a fixed k: **(a)** $k = 0.2$, **(b)** $k = 0.4$.

TABLE 4. Values of β on the curves SN, T, H_1, H_2 (determined numerically), for different values of k.

k	SN	T	H_1	H_2
0.2	0.01213643298	0.01223403509	0.01214424451	0.01522659125
0.4	–	0.02058491228	0.02122560336	0.04466593219

- in region 2, the disease free equilibrium P_0 is unstable and the endemic equilibrium P_2 is an attractor outside region 4, when it exists, and unstable inside region 4;

- in region 3 the disease free equilibrium P_0 is an attractor, the endemic equilibrium P_1 is unstable, while the endemic equilibrium P_2 is an attractor outside region 4 and unstable inside region 4.

The numerical simulations in the examples below illustrate the different scenarios of the evolution for the dynamics of model (2.4), consistent with the theoretical results.

Example 6.1. *For $k = 0.4$ we have considered the following values of β:*
i) $\beta = 0.021$ (between T and H_1);
ii) $\beta = 0.022$ (between H_1 and H_2, close to H_1);
iii) $\beta = 0.042$ (between H_1 and H_2, close to H_2);
iv) $\beta = 0.046$ (close to H_2).

For these values of β and k, the equilibrium point P_0 is unstable. In cases i) and iv) the trajectories of the point $S(0) = 21.945,\ E(0) = 0.129,\ I(0) = 0.132$ are attracted to the equilibrium P_2. See figures 7 and 10.

In cases ii) and iii) the trajectories are attracted to the limit cycles born through the Hopf bifurcation. The corresponding time series for the compartment variables also show a periodic behavior. See Figures 8, 9.

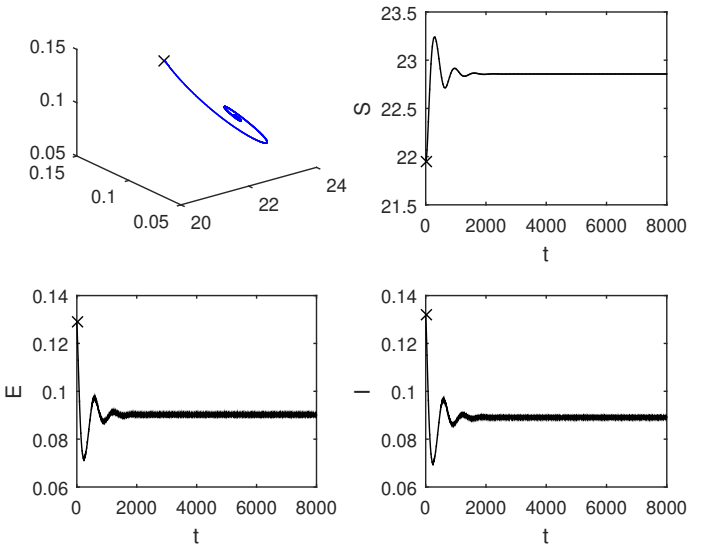

FIGURE 7. Orbit of the point $S(0) = 21.945,\ E(0) = 0.129,\ I(0) = 0.132$ and time series, for $k = 0.4$ and $\beta = 0.021$.

Example 6.2. *For $k = 0.2$ we have considered the following values of β:*
(i) $\beta = 0.012138$ and $\beta = 0.01214$ (between SN and H_1);
(ii) $\beta = 0.0122$ (between H_1 and T);
(iii) $\beta = 0.014$ (between T and H_2, close to H_2);
(iv) $\beta = 0.016$ (close to H_2).
In Figures 11-14 there are represented orbits and time series for four initial points, namely:
- the point $(\frac{A}{\mu} + 0.1, 0, 0.1)$, close to the equilibrium point P_0 (in green);
- the equilibrium point P_2 (in yellow);
- two points close to the P_2 (in red and blue).

In case (i), Figure 11 shows that both P_0 and P_2 are attractors. In case (ii), Figure 12 shows two attractors, namely P_0 and a limit cycles born through a supercritical Hopf bifurcation. In case (iii), both P_0 and P_2 are unstable. Figure 13 shows a stable limit cycle, and the time series for the compartment variables with a periodic behavior. In case (4) (see figure 14), all trajectories of the considered initial points are attracted to the equilibrium P_2.

Remark that, as the system is three-dimensional, strange attractors may also exist. The numerical simulations performed showed no such behavior.

7. CONCLUSIONS

In this paper we proposed and investigated a SEIR type model (2.1), with nonlinear transmission and removal rates. The model generalizes previous investigated SEIR type

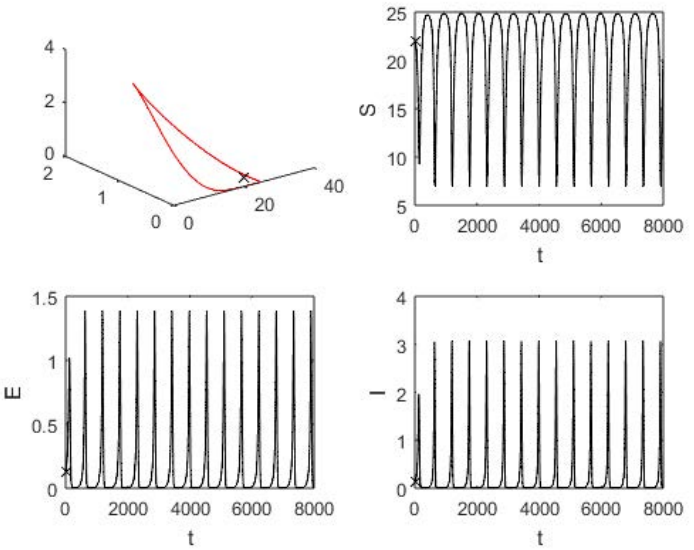

FIGURE 8. Orbit of the point $S(0) = 21.945,\ E(0) = 0.129,\ I(0) = 0.132$ and time series, for $k = 0.4$ and $\beta = 0.022$.

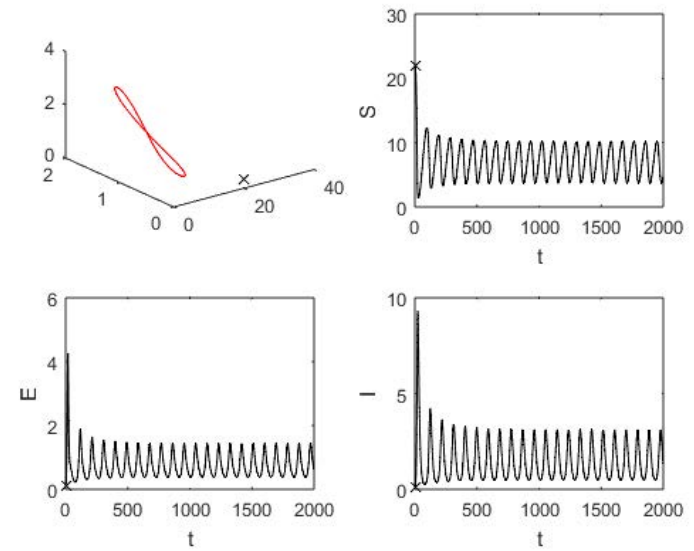

FIGURE 9. Orbit of the point $S(0) = 21.945,\ E(0) = 0.129,\ I(0) = 0.132$ and time series, for $k = 0.4$ and $\beta = 0.042$.

epidemiological models. Analysing the reduced $3D$ associated system (2.4), we proved that the proposed model may have unique or coexisting stable attractors, corresponding to stationary or periodic solutions.

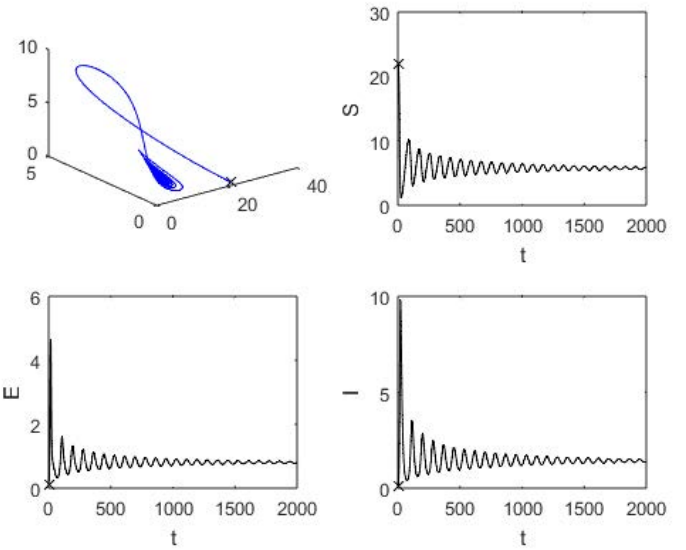

FIGURE 10. Orbit of the point $S(0) = 21.945,\ E(0) = 0.129,\ I(0) = 0.132$ and time series, for $k = 0.4$ and $\beta = 0.046$.

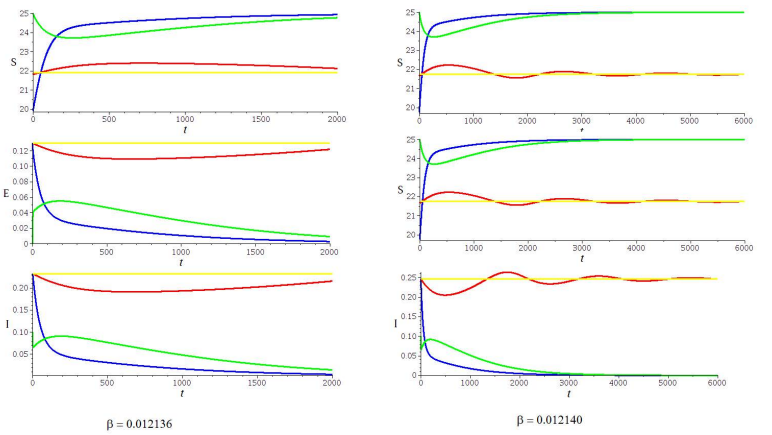

FIGURE 11. Projections of orbits and time series, showing evolution to P_0 or to P_2, for $k = 0.2$ and $\beta = 0.012138$ (to the left), $\beta = 0.01214$ (to the right).

In addition to the disease free equilibrium point, the system may posses one or two endemic equilibria.

If the basic reproduction number R_0 is smaller than 1, the disease free equilibrium is locally asymptotically stable. In addition, if $\frac{d\Phi}{dI}(0) < 1$, there are no endemic equilibria. If $\frac{d\Phi}{dI}(0) > 1$ and $\bar{R} < R_0 < 1$, there exist two endemic equilibria, born through a fold bifurcation. The 'smaller' equilibrium (i.e. the one with I^* closer to 0) is unstable, while the 'larger' one is asymptotically stable for parameters close to the fold bifurcation stratum.

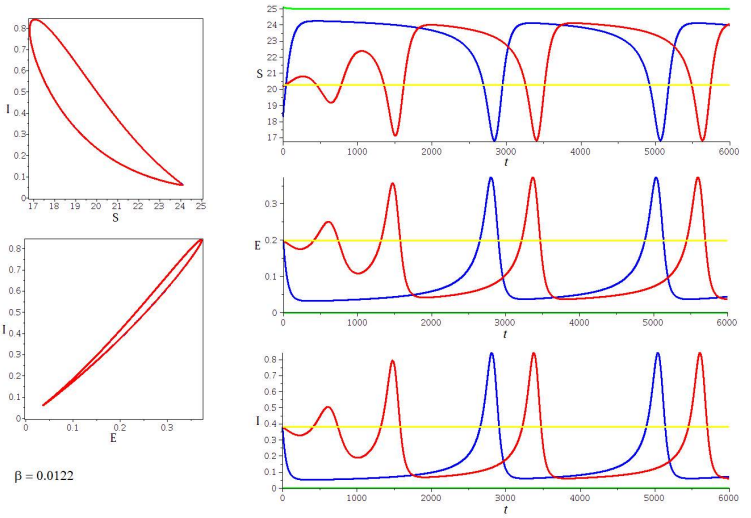

FIGURE 12. Projections of orbits and time series, showing evolution to P_0 or to a limit cycle, for $k = 0.2$ and $\beta = 0.0122$.

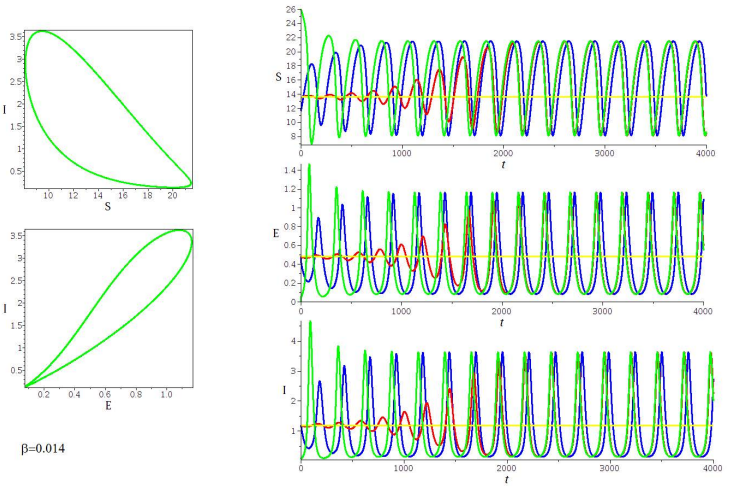

FIGURE 13. Projections of orbits and time series, showing evolution to a limit cycle, for $k = 0.2$ and $\beta = 0.014$.

The stability of the larger equilibrium may change through a Hopf bifurcation. Consequently, for basic reproduction number between $\bar{R}$ and 1, there may coexist two stable equilibria or one stable equilibrium and a stable limit cycle.

If $R_0 > 1$, the disease free equilibrium is unstable and there exists exactly one endemic equilibrium point, which is either stable or may lose stability through a Hopf bifurcation. Thus, the system evolves either to the endemic equilibrium point or to a stable limit cycle, for parameters close the Hopf bifurcation stratum.

In the case study in Section 5, we considered Holling type II response functions for both the transmission and the removal rates. Considering two of the parameters as variables, we have emphasized parameter strata where each of the theoretical scenarios takes place.

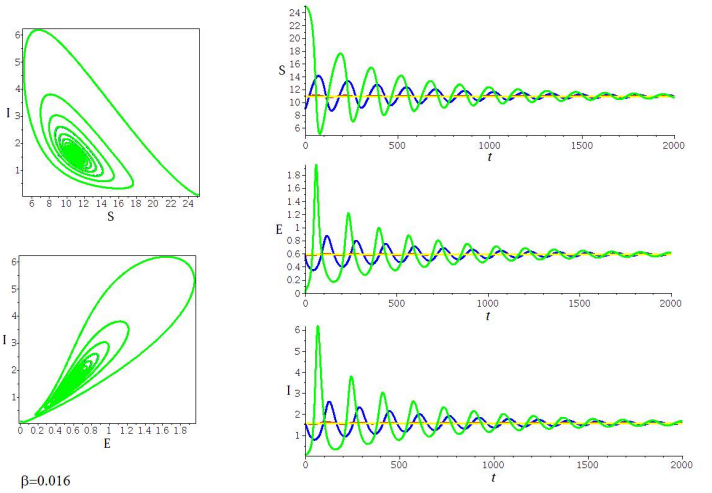

FIGURE 14. Projections of orbits and time series, showing evolution to P_2, for $k = 0.2$ and $\beta = 0.016$.

The theoretical results are confirmed by the numerical ones, obtained by using the MatLab software.

ACKNOWLEDGMENTS

The first two authors were partially supported by 101183111-DSYREKI - HORIZON-MSCA-2023-SE-01: Dynamical Systems and Reaction Kinetics Networks project.

REFERENCES

[1] Capasso, V. *Mathematical Structures of Epidemic Systems.* Springer, Berlin, Heidelberg, 1993.
[2] Capasso, V.; Serio, G. Generalization of the Kermack-Mckendrick Deterministic Epidemic Model. *Math. Biosci.* **42** (1978), no. 1-2, 43-61.
[3] Gómez, M. C.; Mondragon, E. I. Global stability analysis for a SEI model with nonlinear incidence rate and asymptomatic infectious state. *Appl. Math. Comput.* **402** (2021), 126130.
[4] Gumel, A. B.; Moghadas, S. M. A qualitative study of a vaccination model with nonlinear incidence. *Appl. Math. Comput.* **143** (2003), no. 2-3, 409-419.
[5] Hethcote, H. W.; van den Driessche, P. Some epidemiological models with nonlinear incidence. *J. Math. Biol* **29** (1991), 271-287.
[6] Levin, S. A.; Hallam,T. G.; Gross, L. J. *Applied Mathematical Ecology Springer.* Springer, Berlin, Heidelberg, 1989.
[7] Yorke, J. A.; London, W. P. Recurrent outbreaks of measles, chickenpox and mumps. II. Systematic differences in contact rates and stochastic effects. *Am. J. Epidemiol.* **98** (1973), no. 6, 469-82.
[8] Liu Wm.; Hethcote H. W.; Levin, S. A. Dynamical behavior of epidemiological models with nonlinear incidence rates. *J. Math. Biol.* **25** (1987), 359-380.
[9] Liu, Wm.; Levin S.A.; Iwasa, Y. Influence of nonlinear incidence rates upon the behavior of SIRS epidemiological models. *J. Math. Biol.* **23** (1986), 187-204.
[10] van den Driessche, P.; Watmough, J. A simple SIS epidemic model with a backward bifurcation. *J. Math. Biol.* **40** (2000), 525-540.
[11] Moghadas, S. M.; Gumel, A. B. Global stability of a two-stage epidemic model with generalized nonlinear incidence. *Math. Comput. Simul.* **60** (2002), no. 1-2, 107-118.
[12] Ruan, S.; Wendi, W. Dynamical behavior of an epidemic model with a nonlinear incidence rate. *J. Differ. Equ.* **188** (2003), no. 1-2, 135-163.
[13] Castañeda, A. R. S.; Ramirez-Torres, E. E.; Valdés-García, L. E.; Morandeira-Padrón, H. M.; Yanez, D. S.; Montijano, J. I.; Bergues Cabrale, L. E. Modified SEIR epidemic model including asymptomatic and hospitalized cases with correct demographic evolution. *Appl. Math. Comput.* **456** (2023), 128122.

[14] Shao, P.; Shateyi, S. Stability analysis of SEIRS epidemic model with nonlinear incidence rate function. *Math.* **9** (2021), 2644.
[15] Wang, W.; Ruan, S. Bifurcation in an epidemic model with constant removal rate of the infectives. *J. Math. Anal. Appl.* **291** (2004), no. 2, 775-793.
[16] Bai, Z.; Zhou,Y. Existence of two periodic solutions for a non-autonomous SIR epidemic model. *Appl. Math. Model.* **35** (2011), no. 1, 382-391.
[17] Liu, Q. X.; Jin, Z. Formation of spatial patterns in epidemic model with constant removal rate of the infectives. *J. Stat. Mech.* **2007** (2007), no. 5, 05002.
[18] Zhonghua, Z.; Yaohong, S. Qualitative analysis of a SIR epidemic model with saturated treatment rate. *J. Appl. Math. Comput.* **34** (2010), no. 1, 177-194.
[19] Matallana, P. L.; Blanco, A. M.; Bandoni, J. Estimation of domains of attraction in epidemiological models with constant removal rates of infected individuals. *J. Phys. Conf. Ser.* **90** (2007), no. 1, 012052.
[20] Alexander, M. E.; Moghadas, S. M. Periodicity in an epidemic model with a generalized nonlinear incidence *Math. Biosci.* **189** (2006), no. 1, 75-96.
[21] Moghadas, S. M.; Alexander, M. E. Bifurcations of an epidemic model with nonlinear incidence and infection-dependent removal rate. *Math. Med. Biol.* **23** (2006), no. 3, 231-254.
[22] Nagumo, N. Über die Lage der Integralkurven gewöhnlicher Differentialgleichungen. *Proceedings of the Physico-Mathematical Society of Japan* **24** (1942), 551-559.
[23] Blanchini, F. Set invariance in control. *Automatica* **35** (1999), 1747-1767.
[24] van den Driessche, P.; Watmough, J. Reproduction numbers and sub-threshold endemic equilibria for compartmental models of disease transmission. *Math. Biosci.* **180** (2002), no. 1-2, 29-48.
[25] Diekmann, O.; Heesterbeek, J. A. P.; Metz, J. A. J. On the definition and the computation of the basic reproduction ratio R_0 in models for infectious diseases in heterogeneous populations. *J. Math. Biol.* **28** (1990), 365-382.
[26] LaSalle, J. P. Some extensions of Liapunov's second method. *IRE Transactions on Circuit Theory* **7** (1960), no. 4, 520-527.
[27] Hurwitz, A. On the conditions under which an equation has only roots with negative real part. *Math. Ann.* **6** (1985), no. 2, 273-284.
[28] Sotomayor, J. Generic bifurcations of dynamical systems. In: M. M. Peixoto (Ed.) *Dynamical systems. Proceedings of a Symposium Held at the University of Bahia, Salvador, Brasil, July 26–august 1971*. Academic Press, 1973, 561-582.
[29] Perko, L. *Differential Equations and Dynamical Systems*. 3rd Edition. Springer-Verlag, New York, 2001.
[30] Kuznetsov, Y. *Elements of applied bifurcation theory*. 3rd Edition. Springer Science and Business Media, New York, 2004.
[31] Bolker, B. M.; Grenfell, B. T. Chaos and Biological Complexity in Measles Dynamics. *Proc. Biol. Sci.* **251** (1993), no. 1330, 75-81.
[32] Moghadas, S. M. Modelling the effect of imperfect vaccines on disease epidemiology. *Discrete Continuous Dyn. Syst. Ser. B* **4** (2004), no. 4, 999-1012.
[33] Scherer, A., McLean, A. Mathematical models of vaccination. *Br. Med. Bull.* **62** (2002), no. 1, 187-199.

UNIVERSITY OF CRAIOVA
DEPARTMENT OF MATHEMATICS
STR A. I. CUZA NO 13, 200585, CRAIOVA, ROMANIA
Email address: raluca.efrem@edu.ucv.ro

UNIVERSITY OF CRAIOVA
DEPARTMENT OF MATHEMATICS
STR A. I. CUZA NO 13, 200585, CRAIOVA, ROMANIA
Email address: mihaela.sterpu@edu.ucv.ro

UNIVERSITY OF CRAIOVA
DEPARTMENT OF APPLIED MATHEMATICS
STR A. I. CUZA NO 13, 200585, CRAIOVA, ROMANIA
Email address: dana.constantinescu@edu.ucv.ro